

## Radioactivity Evaluation Considering Operation History for Decommissioning Plant

Maeng YoungJae<sup>a\*</sup>, Lee HyunChul<sup>a</sup>, Kim KyungSik<sup>a</sup>, Yoo SungHoon<sup>a</sup>

<sup>a</sup>Korea Reactor Integrity Surveillance Technology, 324-8, Techno 2-ro, Yuseong-gu, Daejeon, Korea 34036

\*Corresponding author: maeng@krist.co.kr

### 1. Introduction

It is very important to evaluate the radioactivity distribution for the decommissioning plant. The precise evaluation of the radioactivity distribution can make it possible to reduce the radioactive waste volume produced from the decommissioning plant. The radioactivity of the structures near the reactor core such as reactor internals, vessel and concrete shield is mainly due to the neutron irradiation, which is known as the neutron activation phenomenon. The activation level is dependent on the neutron flux irradiating to the interested region of the structure and also dependent on the neutron absorption cross section for those materials.

The neutron flux level is basically dependent on the reactor power level and cycle specific fuel loading pattern. And the power level is changeable during the plant life due to plant overhaul, emergent reactor trip, and low power operation, etc.

In this paper, a robust method to precisely evaluate the radioactivity of the decommissioning plant is introduced. The introduced method is verified by comparing with the measurement radioactivity data set from the surveillance capsules for the interested plant.

### 2. Method

#### 2.1 Neutron Activation Based on Operation History

The neutron activation phenomenon is well known and the activity of the product nuclide when product nuclide is produced at the constant rate of R atoms/sec due to the neutron irradiation can be written as[1]

$$A = R(1 - e^{-\lambda t}) \quad (1)$$

where A is activity (Bq) of the product nuclide and  $\lambda$  is decay constant ( $\text{sec}^{-1}$ ) of the product nuclide. In equation (1) production rate R can be written as

$$R = N_0 \int_0^\infty \sigma(E)\phi(E)dE \quad (2)$$

where  $N_0$  is number of target nuclide irradiated by the neutron flux  $\phi(E)$ , and  $\sigma(E)$  is microscopic cross section for the interested activation reaction. If we select  $N_0$  as atom number density (atoms/g), then the activity of equation (1) becomes specific activity (Bq/g).

We can define reaction rate (RR) and it can be written as a summation form as below by using the multi-group cross section and group-wise neutron spectrum.

$$RR = \int_0^\infty \sigma(E)\phi(E)dE = \sum_{j=1}^n \sigma_j\phi_j \quad (3)$$

In many calculations the group-wise neutron spectrum can be calculated by using the neutron transport code, and these neutron spectrums are derived for the entire region of the plant. For example, DORT[2] and RATOTR-M3G[3] produce 47-group neutron flux solution as a result of the neutron transport calculation. In this case the index n of equation (3) will be 47.

If the neutron flux level of equation (3) is changed, the RR will be also changed. Assuming that the neutron flux is constant during the period i, we can get the RR of period i as follow,

$$RR_i = \sum_{j=1}^n \sigma_j\phi_j^i \quad (4)$$

The specific activity of the product nuclide during the first time period will become

$$A_1 = N_0 RR_1 (1 - e^{-\lambda t_1}) \quad (5)$$

During the next time period the specific activity  $A_1$  will be decayed with its own decay constant and new product nuclide will be created and then the specific activity will become

$$A_2 = A_1 e^{-\lambda t_2} + N_0 RR_2 (1 - e^{-\lambda t_2}) \quad (6)$$

And thus, for the i<sup>th</sup> time period the specific activity becomes

$$A_i = A_{i-1} e^{-\lambda t_i} + N_0 RR_i (1 - e^{-\lambda t_i}) \quad (7)$$

All nuclear power plant has its own operation history which is called as a monthly power history. This is a continuous record of monthly averaged core power level relative to the full power. In this paper the time period of equation (7) is selected as one month, thus the index i mean the number of operation months from initial reactor start-up. Fig. 1 shows the monthly averaged core power level of Kori Unit 1 from August 1977 to April 2015, which is total 453 months from initial start-up. As shown in this figure, the reactor power is changed due to plant overhaul, emergent trip, and low power operation, etc.

#### 2.2 Neutron Transport Calculation

The reaction rate of equation (4) can be written as

$$RR_i = \frac{P_i}{P_{ref}} \sum_{j=1}^n \sigma_j \phi_j^{ref} \quad (8)$$

where  $P_i$  is monthly averaged core power level of  $i^{th}$  month,  $P_{ref}$  is core power level equivalent to the full power, and  $\phi_j^{ref}$  is group-wise neutron flux spectrum equivalent to full power.

The group-wise neutron flux ( $\phi_j^{ref}$ ) of equation (8) can be calculated by using neutron transport code, and RAPTOR-M3G[3] was used in this paper.

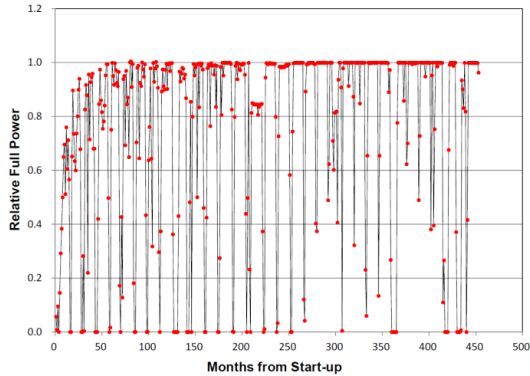


Fig. 1. Monthly Averaged Power Level of Kori-1

One of the important factors affecting radioactivity evaluation is cycle specific fuel loading pattern. Even though the core power levels are same equivalent to the full power for the different cycles, the neutron flux level of the interested region might be changed due to the fuel loading patterns. For the low leakage loading pattern, the flux level of interested region such as vessel is relatively low compared to the high leakage loading pattern. Therefore The group-wise neutron flux ( $\phi_j^{ref}$ ) of equation (8) should be calculated for each cycle.

In this paper RAPTOR-M3G code was used to calculate group-wise neutron spectrum for 3-dimensional geometry from cycle 1 to cycle 30 of Kori Unit 1.

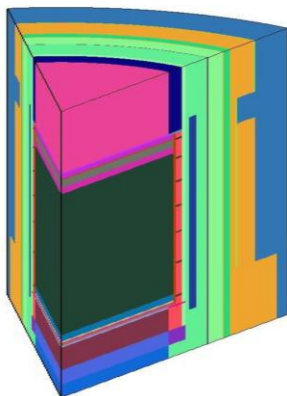


Fig. 2. 3-D Modeling of RAPTOR-M3G for Kori-1

Fig. 2 shows the 3-dimensional RAPTOR-M3G model for Kori Unit 1. In order to run the RAPTOR-M3G code for each cycle, cycle specific radial and axial power distributions information from the nuclear design

report were used. Cycle specific transport calculations were carried out using BUGLE-96 cross-section library [4]. The BUGLE-96 library provides a 67 group coupled neutron-gamma ray cross-section data set (47 groups for neutron, 20 groups for gamma) produced specifically for light water reactor application. In these calculations, anisotropic scattering was treated with a  $P_3$  legendre expansion and the angular discretization was modeled with an  $S_{10}$  order of angular quadrature.

And then the group-wise neutron spectrum data can be calculated for whole geometry including surveillance capsules which contained the neutron dosimeters.

Total six surveillance capsules were installed in Kori Unit 1, and these capsules were irradiated from initial operation and then withdrawn and tested according to the surveillance program. Neutron dosimeter sets were also included in the capsules along with various mechanical test specimens and these dosimeters were activated during the irradiation periods. These measured activity data sets of dosimeters can be used to verify the methods introduced in this paper.

### 3. Results and Conclusion

As described in Section 2, there are 6 measured activity data sets from the 6 surveillance capsules of Kori Unit 1. In this paper measured activities from 5<sup>th</sup> and 6<sup>th</sup> surveillance capsules were selected to compare with calculation results. Table 1 shows the radiological characteristics of each dosimeter used in this paper.

Table 1: Radiological Characteristics of Dosimeters

Sensor Material	Reaction of Interest	Target Atom Fraction	Product Half-Life
Copper	$^{63}\text{Cu}(n,\alpha)^{60}\text{Co}$	0.6917	5.271 year
Iron	$^{54}\text{Fe}(n,p)^{54}\text{Mn}$	0.0585	312.1 day
Nickel	$^{58}\text{Ni}(n,p)^{58}\text{Co}$	0.6808	70.82 day

The 5<sup>th</sup> surveillance capsule was irradiated from the beginning of cycle 1 to the end of cycle 17 in the capsule holder of 23°. On the other hand the 6<sup>th</sup> surveillance capsule was irradiated from the beginning of cycle 1 to the end of cycle 21 in the capsule holder of 33°, and then withdrawn to be stored in the spent fuel pool. This capsule was re-installed in 13° holder at the beginning of cycle 28 and then finally withdrawn and tested at the end of cycle 30.

For the case of the group-wise microscopic cross section ( $\sigma_j$ ) of equation (8), BUGLE-96[4] cross section were used for each reaction. By using equations (7) and (8) the activities of  $^{60}\text{Co}$ ,  $^{54}\text{Mn}$ , and  $^{58}\text{Co}$  were evaluated according to the irradiation period (each month) from initial operation to the last month of irradiation. Figs. 3 thru 5 show  $^{60}\text{Co}$ ,  $^{54}\text{Mn}$ , and  $^{58}\text{Co}$  activity trend of 5<sup>th</sup> capsule, respectively. Figs. 6 thru 8 show  $^{60}\text{Co}$ ,  $^{54}\text{Mn}$ , and  $^{58}\text{Co}$  activity trend of 6<sup>th</sup> capsule, respectively.

Note that the 6<sup>th</sup> surveillance capsule has been stored and decayed in the spent fuel pool without irradiation from cycle 22 to cycle 27.

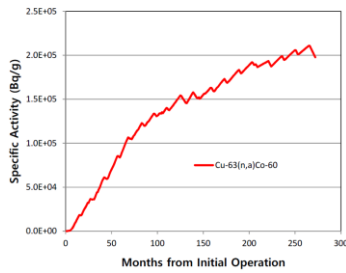


Fig. 3. <sup>60</sup>Co Activity Trends for Kori-1 5<sup>th</sup> Capsule



Fig. 4. <sup>54</sup>Mn Activity Trends for Kori-1 5<sup>th</sup> Capsule

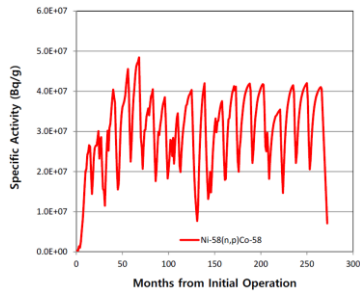


Fig. 5. <sup>58</sup>Co Activity Trends for Kori-1 5<sup>th</sup> Capsule

As shown in these figures the specific activities of the product nuclides are increasing during the first period of irradiation, and then decreasing during the overhaul period. The specific activity trend of <sup>58</sup>Co which was created by the reaction of <sup>58</sup>Ni(n,p)<sup>58</sup>Co is very changeable according to the power level. That is because of the relatively small decay constant of <sup>58</sup>Co.

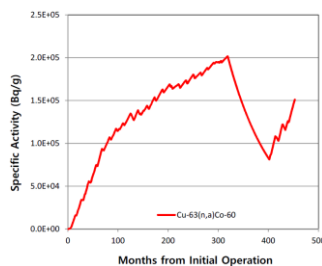


Fig. 6. <sup>60</sup>Co Activity Trends for Kori-1 6<sup>th</sup> Capsule

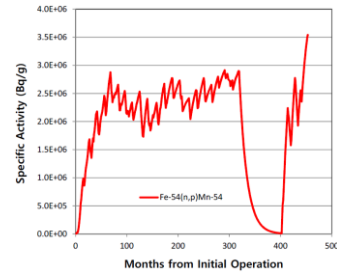


Fig. 7. <sup>54</sup>Mn Activity Trends for Kori-1 6<sup>th</sup> Capsule

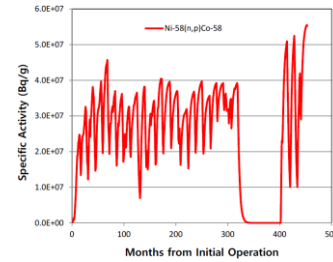


Fig. 8. <sup>58</sup>Co Activity Trends for Kori-1 6<sup>th</sup> Capsule

Table 2 shows the comparisons between calculated and measured specific activities for each dosimeter. The % error is derived as  $(C-M)/M \times 100$ , where C and M are calculated and measured specific activities respectively. As shown in this table, there are very good agreement between calculation and measurement. Therefore the methods introduced in this paper can be used for the precise evaluation of the radioactivity of the radioactive waste of the decommissioning nuclear power plant.

Table 2: Calculation and Measurement Comparison

Caps.	Reaction	Spec. Activity (Bq/g)		% error
		Calc.	Meas.	
5 <sup>th</sup>	<sup>63</sup> Cu(n,α) <sup>60</sup> Co	1.98E+05	1.99E+05	-0.50
	<sup>54</sup> Fe(n,p) <sup>54</sup> Mn	2.01E+06	1.94E+06	3.61
	<sup>58</sup> Ni(n,p) <sup>58</sup> Co	7.10E+06	7.14E+06	-0.56
6 <sup>th</sup>	<sup>63</sup> Cu(n,α) <sup>60</sup> Co	1.51E+05	1.55E+05	-2.58
	<sup>54</sup> Fe(n,p) <sup>54</sup> Mn	3.54E+06	3.33E+06	6.31
	<sup>58</sup> Ni(n,p) <sup>58</sup> Co	5.53E+07	5.64E+07	-1.95

## REFERENCES

- [1] John R. Lamarsh, Introduction to Nuclear Engineering, 3rd ed. Pearson, 2001, Chapter 2.
- [2] RSIC Computer Code Collection CCC-650, "DOORS 3.1, One-Two and Three Dimensional Discrete Ordinates Neutron/Photon Transport Code System," August 1996.
- [3] Westinghouse, LTR-REA-11-65, Rev. 0 "RAPTOR-M3G Version 2.0 User Manual", November 3, 2011.
- [4] RSIC Data Library Collection DLC-185, "BUGLE-96, Coupled 47 Neutron, 20 Gamma-Ray Group Cross-Section Library Derived from ENDF/B-VI for LWR shielding and Pressure Vessel Dosimetry Applications," March 1996.